

This manuscript has been authored by UT-Battelle, LLC under Contract No. DE-AC05-00OR22725 with the U.S. Department of Energy. The United States Government retains and the publisher, by accepting the article for publication, acknowledges that the United States Government retains a non-exclusive, paid-up, irrevocable, worldwide license to publish or reproduce the published form of this manuscript, or allow others to do so, for United States Government purposes. The Department of Energy will provide public access to these results of federally sponsored research in accordance with the DOE Public Access Plan (<http://energy.gov/downloads/doe-public-access-plan>).

Cooperative atomic motion during shear deformation in metallic glass

Yoshinori Shiihara,^{1,*} Takuya Iwashita,^{2,†} Nozumu
Adachi,³ Yoshikazu Todaka,³ and Takeshi Egami^{4,5,‡}

¹*Graduate School of Engineering, Toyota Technological
Institute, Nagoya, Aichi 468-8511, Japan*

²*Department of Integrated Science and Technology,
Oita University, Oita 870-1192, Japan*

³*Department of Mechanical Engineering,
Toyohashi University of Technology, Toyohashi, Aichi 441-8580, Japan*

⁴*Department of Materials Science and Engineering
and Department of Physics and Astronomy,
University of Tennessee, Knoxville, Tennessee 37996, USA*

⁵*Materials Science and Technology Division,
Oak Ridge National Laboratory, Oak Ridge, Tennessee 37831, USA*

(Dated: March 20, 2025)

Abstract

Elucidating mechanical deformation in glassy materials at the atomic level is challenging due to their disordered atomic structure. Using our novel “frozen atom analysis” of the simulation data, we reveal that anelastic deformation in CuZr metallic glasses is fundamentally driven by cooperative atomic motions of approximately 40 elastically linked atoms, forming trigger groups. They initiate localized rearrangements, which can cascade into plastic flow. Notably, these groups show no distinct structural or physical features, challenging the idea that deformation occurs in defective regions. Instead, deformation events are highly stochastic and transient, driven by collective atomic motion. This finding not only reshapes our understanding of glassy material deformation mechanisms but also highlights cooperative motion as a key factor in avalanche-like phenomena governing the behavior of disordered systems across multiple scales.

* shiihara@toyota-ti.ac.jp

† tiwashita@oita-u.ac.jp

‡ egami@utk.edu

Unraveling the microscopic mechanisms behind plastic and anelastic deformation in glassy materials, such as metallic glasses, remains an enduring mystery over half a century[1–3]. In crystalline materials, lattice defects, such as dislocations, are carriers of plasticity, playing a crucial role in determining mechanical properties. However, the absence of long-range atomic order in glassy materials makes it difficult to define defects. Moreover, in crystals, dislocation density and pinning effects are highly sensitive to microstructural variations, leading to significant differences in mechanical strength[4, 5]. In contrast, metallic glasses display remarkably universal mechanical responses across different compositions and processing conditions[6], suggesting that the conventional paradigm linking structural defects to mechanical behavior may not directly apply to metallic glasses. This raises fundamental questions: if defects are not the primary deformation carriers, what governs mechanical behavior in glassy materials? Identifying these underlying mechanisms could lead to a more comprehensive understanding of deformation behavior in strongly disordered solids.

We show, through computational simulations of shear deformation in metallic glasses, that the fundamental deformation elements in these materials are atomic groups exhibiting cooperative motion. Numerous studies have investigated atomic cooperativity in glasses and supercooled liquids, both under applied stress[7–11] and in stress-free conditions[12–17]. Yet, even in simulations, cooperative movements have thus far been inferred only from the displacements of atomic groups during stress relaxation events. A widely used framework for describing the plastic deformation of metallic glasses is based on Shear Transformation Zones (STZs), which are localized, collective atomic rearrangements[6, 7, 9, 18]. In the framework of self-organized criticality, the interaction and propagation of STZs in an avalanche-like manner have been widely discussed[19–21]. These discussions suggest that plastic deformation is governed by strongly interacting elements exhibiting collective behavior across multiple length scales. However, a detailed microscopic understanding of these processes—particularly the triggers for deformation events and the nature of their interactions—remains incomplete. We identified this cooperative behavior as the essential core of STZs, which we refer to as the “STZ core.” We analyze their size, structural, and mechanical characteristics, while also revealing the presence of cascading STZ cores that initiate the early stages of avalanches. This analysis enhances the understanding of deformation mechanisms in metallic glasses and other amorphous materials.

Cooperativity in glassy materials is concealed within their complex atomic dynamics,

making its extraction challenging. To address this, we introduce frozen atom analysis, a novel computational technique that explores “what-if” scenario. In real life it is impossible to go back in time, but in simulation we can trace the time back, like in a time-machine, and change history. We identify a local plastic deformation event, and go back in time to the instance just before the start of the event. Then we artificially immobilize an individual atom. If this atom is involved in cooperative motion, the deformation event will not happen when the simulation is continued with the atom immobilized. We applied this “if” condition to each atom in the system and identify the atoms involved in cooperative motion, thereby revealing the STZ core. Through the comparison of “parallel worlds” enabled by frozen atom analysis, we uncover the fundamental nature of STZs, distinct from the conventional perspectives which rely upon the post-mortem analysis of the event. We found that the STZ core consists of an average of 40 atoms, which engage in cooperative motion. These atoms lack distinct structural features, suggesting that the STZ core can emerge anywhere. Furthermore, it induces plastic deformation among the surrounding atoms and acts as a trigger, initiating cascades that drive avalanches. These findings represent a drastic departure from the conventional view that STZs correspond to defects or soft spots, paving the way toward deeper insights into the physical principles governing the deformation mechanisms of glassy materials.

RESULTS

Frozen atom analysis

The frozen atom analysis enables the unambiguous identification of atomic groups involved in cooperative motion, specifically STZ cores. The Athermal Quasi-Static (AQS) method[22, 23] is a widely used computational approach for modeling critical slip phenomena under quasi-static shear in glassy materials. In this method, a model glass undergoes incremental affine shear deformation, followed by athermal relaxation, transitioning through mechanically stable configurations. A characteristic feature of this process is the sudden shear stress drop during relaxation, signaling a plastic deformation event involving atomic rearrangements (Fig. 1a). Frozen atom analysis is applied at this critical stress drop to pinpoint the STZ core. The method starts from the atomic configuration just before the

deformation event, applies an affine deformation, and artificially “freezes” one atom while allowing the rest to relax. If the plastic deformation event does not occur, the frozen atom is identified as a part of the STZ core, confirming its essential role in the deformation event. As conceptually illustrated in Fig. 1b, freezing an atom disrupts the cooperative movement of the entire group, highlighting their interdependence.

We implement this method as follows: during the relaxation process of a stress-drop event in the AQS procedure, one atom from a system of n atoms is selected, and its motion is artificially frozen. The remaining atoms are allowed to relax, and the total displacement of the entire system is recorded. This is referred to as the D_f parameter (in Å) here.

$$D_f = \sqrt{\sum_{i=1}^N \|\mathbf{d}_i\|^2}, \quad (1)$$

where \mathbf{d}_i represents the displacement vector of atom i during the structural relaxation. This process is repeated for every atom, generating a D_f parameter value for each atom. This D_f parameter clearly distinguishes between atoms that participate in cooperative motion and those that do not: a D_f value of zero indicates that freezing the atom’s motion disrupts the cooperative displacement, showing that the atom with $D_f = 0$ is a part of the deformation element. Conversely, a non-zero D_f value indicates that the atom’s displacement is not critical to the cooperative motion. This method is related to the atomic pinning approach to probe atomic cooperativity in flow[24], but here atomic freezing is used merely to probe the role of each atom in deformation, and it does not affect the flow itself.

In conventional simulations and experiments, pinpointing the atomic-level interactions or mechanisms that drive observed plastic deformation can be challenging. By deliberately controlling the motion of specific atoms, frozen atom analysis enables us to virtually modify their movements and directly probe causal relationships. Comparing multiple “parallel worlds,” where different atoms are immobilized, makes it possible to extract the hidden cooperative motion embedded within the disordered structure of glassy materials.

Identification of atomic group in cooperative motion

The histogram of the D_f parameter obtained from a stress-drop event is shown in Fig.1c as an example, from which three groups of atoms can be extracted, as illustrated on the right side of the figure. The first group consists of atoms with D_f values close to zero (visualized

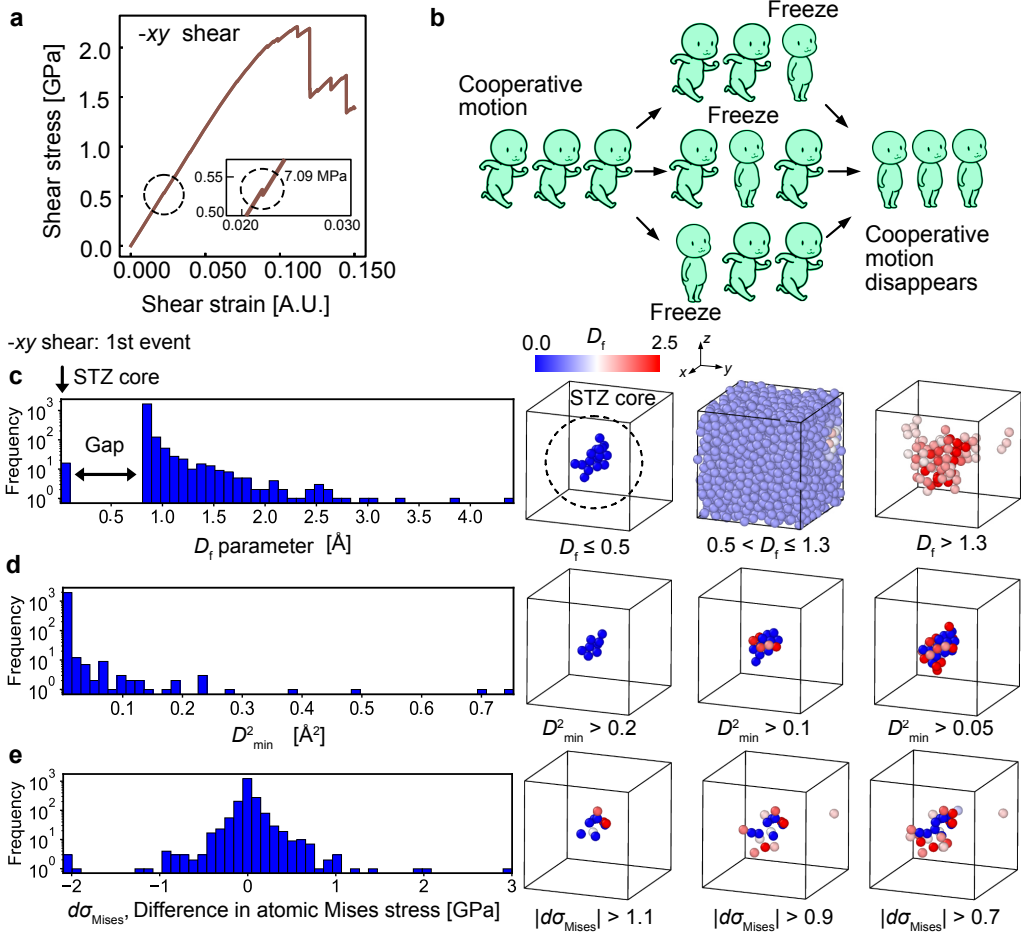


FIG. 1. Frozen atom analysis in metallic glass: **a**, Stress-strain curve of metallic glass obtained from AQS simulations in $-xy$ shear direction. The plastic event to which frozen atom analysis is applied is marked with a dashed circle. The inset zooms in on the stress drop associated with the event, showing a decrease of approximately 7.1 MPa. **b**, Conceptual illustration of frozen atom analysis. Cooperative motion is illustrated by a group of people walking together, where freezing one individual restricts others. Stopping the front person blocks those behind, freezing the middle constrains both sides, and immobilizing the back pulls the front individuals backward. This analogy captures the cooperative nature of atomic rearrangements in metallic glasses. **c-e**, Logarithmic histograms comparing different shear transformation zone (STZ) descriptors for the first stress relaxation event. **c**, The D_f parameter obtained from frozen atom analysis. **d**, The non-affine displacement metric D_{\min}^2 . **e**, The difference in atomic von Mises stress before and after the event. The right panels visualize atoms with descriptor values in specific ranges using OVITO software[25], where atoms are color-coded based on the D_f parameter.

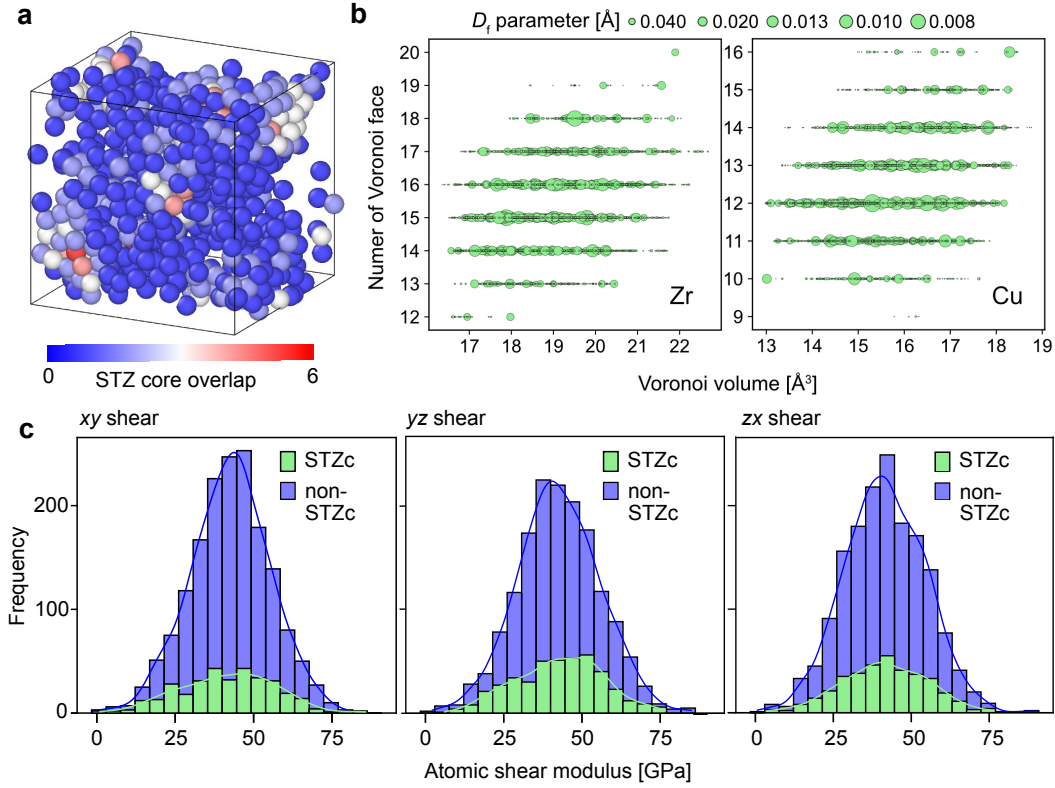


FIG. 2. Characteristics of STZ core: **a** Atomic configurations identified as STZ cores in 36 deformation events. The color represents the frequency with which atoms were classified as STZ cores across multiple events. **b** Comparison of Voronoi features (number of Voronoi faces and Voronoi volume per atom) and D_f parameters for Zr (left) and Cu (right). Larger circles represent atoms with larger D_f values, indicating that they are more involved in cooperative motion. **c** Histograms of the atomic shear modulus for STZ core atoms (STZc) and non-core atoms (non-STZc). The atomic shear modulus corresponding to each shear direction is shown. The STZ cores considered are those driven by deformation along the respective shear direction. The modulus is calculated as the analytic derivative of the Embedded Atom Method (EAM) potential with respect to cell strain[26].

as $D_f \leq 0.5$ in the figure on the right). As mentioned earlier, these are the atoms frozen during the relaxation process halt the motion of other atoms. In other words, this group represents atoms critically needed for cooperative motion. As shown in the Methods section, such cooperative motion was observed in all 36 stress relaxation events investigated in this study. Therefore, it can be concluded that all STZ cores observed here are the atomic groups

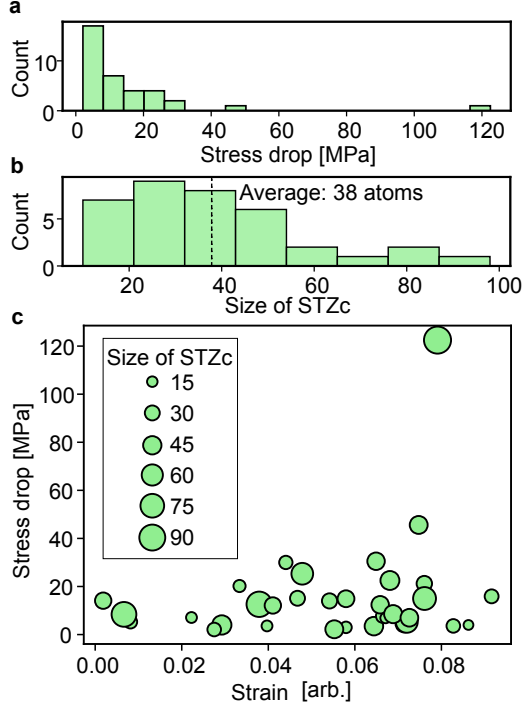


FIG. 3. Event size and corresponding STZ core (STZc) size in 36 stress-drop events: **a**, Histogram of stress-drop magnitudes. **b**, Histogram of the number of atoms included in the STZ core. **c**, Relationship between the applied shear strain on the cell and the stress-drop magnitude. The size of the circles is proportional to the number of atoms in the STZ core observed during each event.

critical for cooperative motion.

The second group of atoms is located near the peak of the histogram. Even when their motion is frozen, the cooperative motion appears during the relaxation process, meaning they are not directly involved in the activation of the deformation event. The peak position of the histogram corresponds to the D_f value when no atoms are frozen. As shown in the figure on the right ($0.5 < D_f \leq 1.3$ case), most atoms in the system belong to this group. The third group, found in the tail of the histogram and located near the STZ group ($D_f > 1.3$ case), experiences large displacements due to cooperative motion but does not affect the deformation event. When their motion is frozen, all other atoms move to reproduce the original displacement, leading to large D_f values for this group, indicating that they do not stop the cooperative motion.

A remarkable feature of the D_f parameter lies in the gap observed in the histogram. As shown in Figure 1c, this gap clearly distinguishes the group of atoms belonging to the

STZ core, which exhibit cooperative motion, from other atoms. Similar attempts using the traditional indicators (see the Methods section), non-affine displacement metric, D_{\min}^2 , and the difference in atomic von Mises stress during relaxation are shown in Figures 1d and 1e. The atoms identified by various methods largely overlap with each other, proving that they arrive at similar conclusions. The sizes of the STZ cores obtained in this study were fewer than 100 atoms, with an average of about 40 atoms, which is consistent with the sizes of STZs reported in previous studies[1]. However, in previous studies the number of atoms constituting the STZ depends on arbitrary parameters, such as the threshold value. In contrast, the frozen atom method with the D_f parameter identifies the STZ core without ambiguity.

Characteristics of STZ core

The characteristics of STZs, including their size, shape, distribution, and hardness, have been subjects of long-standing debate[1, 27]. We studied the atomic level characteristics of the STZ core atoms at the initial stage before the stress was applied. The nature of the STZs identified in this study differs significantly from those previously discussed. Figure 2a illustrates the spatial distribution of STZ cores detected in the 36 events considered. These STZ cores are widely spread across the system, indicating that STZ cores do not form in a spatially confined region but rather emerge throughout the material. The low occurrence of overlaps suggests that these events rarely occur repeatedly in the same locations. Figure 2b plots the features of Voronoi polyhedra, specifically the number of faces and the volume, for the 72,000 atoms considered in this calculation. Despite the widespread use of Voronoi polyhedra as descriptors for characterizing the atomic structure of defects, including STZs, the nearly uniform distribution of atoms with low D_f values within the STZs suggests that extracting STZs based solely on Voronoi features may not be a reliable approach. Figure 2c compares histograms of atomic shear modulus for STZ core atoms detected in each shear direction with those of non-core atoms. The obtained histograms and modulus values are consistent with those reported in previous studies[26, 28]. No significant difference in hardness was observed between STZ core atoms and other atoms. This indicates that STZ cores are neither the “soft spots” as traditionally perceived nor “hard spots”; in other words, they do not exhibit any distinct characteristics in terms of hardness. In the Methods section,

we present the evolution of average atomic energy and von Mises stress within each STZ core during the AQS process. Even within the apparent elastic regime, energy and stress responses exhibit strong variation with applied stress. This indicates that the mechanical response of this system is highly nonlinear, and atoms are significantly influenced by interactions with other activated STZ cores. This underscores the role of intrinsic structural inhomogeneity in driving localized structural and mechanical changes under external stimuli, challenging predictions based on the initial state.

Figure 3 explores the relationship between the STZ core size and the magnitude of stress drops observed in the 36 events considered. The histogram of stress drop magnitude follows a power-law distribution (Fig. 3a), whereas the histogram of the STZ core differs from it, exhibiting a shape similar to a Poisson distribution (Fig. 3b). Whereas it is widely believed that the size of the STZ is proportional to the magnitude of the stress drop, the histograms of stress-drop magnitude and STZ core size in this study show otherwise. Even though some correlations are found in Fig. 3c between the magnitude of stress drop and the macroscopic strain at which the event occurred, the size of the STZ core has no correlation with either.

These results suggest that the atoms in STZ cores are not in special environments that could be identified as defects, in agreement with the earlier study[29]. It is likely that any atom can be involved in STZ cores. This may explain why the critical strength is so universal among various metallic glasses[6].

Local configurational excitation in STZ core

To further examine the nature of the STZ core thus defined at the atomic level, we investigated the Local Configurational Excitation (LCE) that occurs during the stress-drop process. LCE refers to the action of losing or gaining nearest-neighbor atoms around a particular atom. This change in the atomic connectivity network due to bond switching is known to govern the macroscopic viscosity of high-temperature liquids (details are provided in Ref.[30] and the Methods section). Figure 4a compares the number of bond formations and breakages that occur in a single atom during the stress relaxation process between STZ core atoms and non-STZ core atoms. It was found that most LCEs involving three or more bond breakages occur in atoms belonging to the STZ core.

We observe that many atoms in the close vicinity of the STZ core are also displaced due

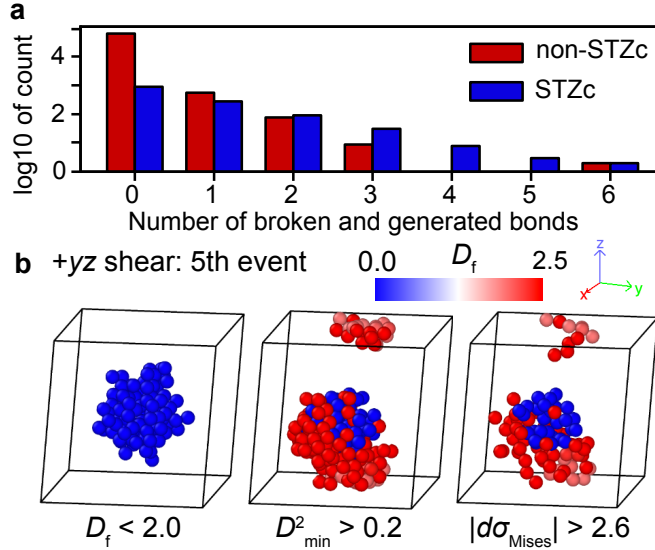


FIG. 4. **a**, Relationship between LCE and STZ core (STZc): A logarithmic histogram for the sum of broken and newly formed bonds for a total of 72,000 atoms involved in the 36 stress relaxation events considered in this study. **b**, Visualization of the STZ core that triggered events containing non-STZ core atoms with six broken and generated bonds (5th event in yz shear direction with 122.49 MPa stress drop), using each descriptor. Atoms are color-coded based on the D_f parameter.

to the activation of the core, as exemplified by the third atom group with $D_f > 1.3$ in Fig. 1c. LCEs that occur in the STZ core induce non-affine displacements in its surroundings, and these displacements can sometimes drive other STZ cores. Figure 4a shows that some atoms, despite being classified as non-STZ core, exhibit a significant number of LCEs. Figure 4b illustrates the corresponding event. While the D_f parameter identifies a STZ core, other parameters suggest that other atoms in the vicinity are also involved in the deformation event. Of the atoms involved in LCE, only 55% are included in the STZ core, while the remainder are either surrounding the STZ core or part of events triggered by the core. The LCE analysis revealed that five out of the 36 events considered exhibited cascade-like behavior (see the Methods section for details). These results imply that the activation of one STZ core triggers a local avalanche of deformation, which is more extended and involves a larger number of atoms. The deformation event, or the STZ, is complex, and involves the trigger and subsequent large local deformation in its vicinity. This was made clear for the first time due to the frozen atom analysis which enabled a clear distinction between triggering and triggered STZ regions.

DISCUSSION

The differences in the characteristics of STZs between previous studies and this study originate from differing interpretations of the STZ concept. In prior research, physical quantities such as D_{\min}^2 , which have been used to identify STZs, primarily reflect the a posteriori consequences of STZ activation. Therefore, STZs are defined as the result of the deformation event rather than the dynamic phenomenon as a whole. Based on this interpretation, it is natural to expect a proportional relationship between the size of the stress drop and the size of the STZ. In contrast, in this study, the STZ core is defined in the a priori state in terms of the eventual contribution to the deformation event. To be specific, STZ cores are defined as atomic groups that relax stress through cooperative motion, and this definition is made for the state prior to the deformation event. The analysis of the characteristics of individual atoms in STZ cores reveal that the formation of STZ cores is a highly stochastic and transient process: unlike conventional deformation units such as dislocations, they do not possess distinct structural features and can form anywhere. It is possible that local factors other than defective atomic structures, such as elastic and strain heterogeneities within a disordered structure, lead to local deformation events. But the analysis of the nature of the STZ core atoms just prior to the deformation events did not expose any particular characteristics, either. STZs are statistically created and disappear after deformation events, as presumed in the STZ theory by Langer[31].

Furthermore, contrary to the widely spread idea of the STZ as the site of massive liquid-like flow, the number of atomic bond breakings is rather small. Only 34% of atoms in the STZ core are involved in LCE. Instead, the STZ core functions as a trigger, where atoms move cooperatively as an elastically bound group, initiating large-scale deformation. On average, approximately 40 atoms play a crucial role in deformation, collectively constraining each other's motion. This elastic nature of STZ cores contrasts with the conventional soft spot interpretation, which assumes localized regions of structural weakness. While STZ cores are not hard spots either, their deformation behavior emerges nonlinearly rather than being determined solely by pre-existing spatial heterogeneity. The presence of elastically bound groups in deformation is consistent with our earlier observation of transient solid-like groups of atoms during shear flow[32], further supporting the idea that STZs are distinct from pre-defined defects.

A key finding of this study is that STZ cores do not exhibit unique structural features in their initial state, making them inherently unpredictable based on conventional descriptors such as Voronoi volume, atomic stress state, or atomic shear modulus. Unlike defects that can be identified from static configurations, STZ cores emerge dynamically through cooperative atomic motion in response to the nonlinear stress and strain behavior of a glassy structure under external stimuli. This suggests that local configurational excitations (LCEs) and the activation of STZ cores are not predetermined but rather a consequence of evolving interactions. Furthermore, one STZ core can drive another, leading to cascading deformation events. This indicates that deformation is not solely dictated by isolated activation sites but also by interactions between STZ cores and their surrounding environment.

The STZ core was identified by the frozen atom analysis, which functions as a “time machine” to explore parallel histories of atomic motion. While conventional methods focus on analyzing characteristic deformation units and lattice defects, this technique enables the systematic isolation of fundamental triggers of plastic deformation by freezing specific atoms and tracing their impact. The scenario presented by this analysis is as follows. First, the STZ core is activated as a unit of cooperative motion. The location of STZ cores is unpredictable. Each STZ core involves atomic bond rearrangement, specifically Local Configurational Excitation (LCE), which generates non-affine deformation in the surrounding region. This non-affine deformation, in turn, drives other STZ cores, leading to a cascade of deformation events. These characteristics align with the Self-Organized Criticality (SOC) model, where small perturbations occurring anywhere in space naturally evolve into a critical state that triggers cascading events. This process gives rise to avalanche dynamics observed across different scales in various phenomena[20, 33–35]. In the mathematical model, the emergence of SOC-like behavior depends on the conditions for trigger formation and their interactions[19]. Identifying STZ cores and their cooperative motion can advance the quantitative understanding of SOC in glassy materials, providing key parameters-such as trigger size, spatial distribution, external driving conditions, and their interaction-that serve as a foundation for integrating SOC models into material design. Furthermore, considering the universality of avalanche dynamics, our findings suggest that cooperative motion may serve as a fundamental mechanism underlying SOC behavior in a broad range of nonequilibrium systems.

In conclusion, this study reveals that the fundamental deformation unit in metallic glasses

is made of two components, a trigger and subsequent deformation. We define this atomic group as the STZ core, which has an average size of approximately 40 atoms. This number may vary across different glass systems. However, the frozen atom analysis can determine this number without ambiguity. This cooperative atomic motion functions as the trigger for local deformation events, involving a larger number of surrounding atoms in the process. The absence of distinctive local structural characteristics for the STZ core atoms suggests that STZ cores are not structural defects and can form anywhere in response to external stimuli. These findings challenge the conventional understanding of this complex phenomenon and advance the elucidation of deformation mechanisms in glassy materials. From a broader perspective, the concept established in this study-that cooperative motion serves as the trigger for avalanche-like deformation-has the potential to bridge the understanding of plastic deformation in glassy materials with a wide range of nonequilibrium and nonlinear response systems, where avalanche dynamics play a crucial role. The insights gained in this study are expected to serve as a foundation for their further exploration and deeper understanding.

METHODS

Simulation Setup

We conducted quasi-static shear deformation on a periodic three-dimensional metallic glass $\text{Cu}_{50}\text{Zr}_{50}$, comprising 2000 atoms. The molecular dynamics simulations were carried out using the LAMMPS software package[36] with the Embedded Atom Method (EAM) potential for Cu-Zr[37]. The metallic glass was prepared by melting and cooling a B2 alloy of CuZr. First, a velocity distribution corresponding to 2000 K was applied to the B2 alloy, and it was cooled to 0 K at a rate of 10^9 K/sec in an nvt ensemble using the Nosé-Hoover thermostat[38, 39]. Subsequently, the atomic structure and cell were relaxed structurally using the steepest descent method, reducing all cell stress components to below 0.1 MPa. The Athermal QuasiStatic (AQS) method[22, 23] was then employed to apply quasi-static shear deformation. This involved applying a small shear strain to the cell vectors of the glass and affinely deforming the atomic structure in accordance with the strain. The configuration was then further relaxed by the steepest descent method to ensure zero force on all atoms. This procedure was repeated 3000 times to induce deformation until the engineering shear strain reached 15%. A total of 36 events were sampled, including six events for each of the six shear directions ($\pm xy$, $\pm yz$, $\pm zx$) as shown in Fig. 5.

Frozen atom analysis to identify STZ core

Various models, such as the Shear Transformation Zone (STZ) model[6, 7, 9, 18], have been proposed to describe deformation behavior, and a number of attempts have been made to identify the deformation mechanism through molecular dynamics simulations[23, 40–45]. In the typical approach, the AQS method, incremental uniform (affine) shear deformation is applied to a model glass structure, and the atomic structure is relaxed athermally at each deformation step. When the shear stress drops during the relaxation, it is assumed that a plastic deformation event occurs through some rearrangement in atomic configuration. For convenience, we call the area with strong plastic deformation an STZ. The changes in certain geometric or physical quantities before and after the relaxation are used to extract features of local atomic behavior. To identify the STZ various metrics have been introduced. These include the non-affine squared displacement (D_{\min}^2)[18, 43, 46], Voronoi-based metrics[47, 48],

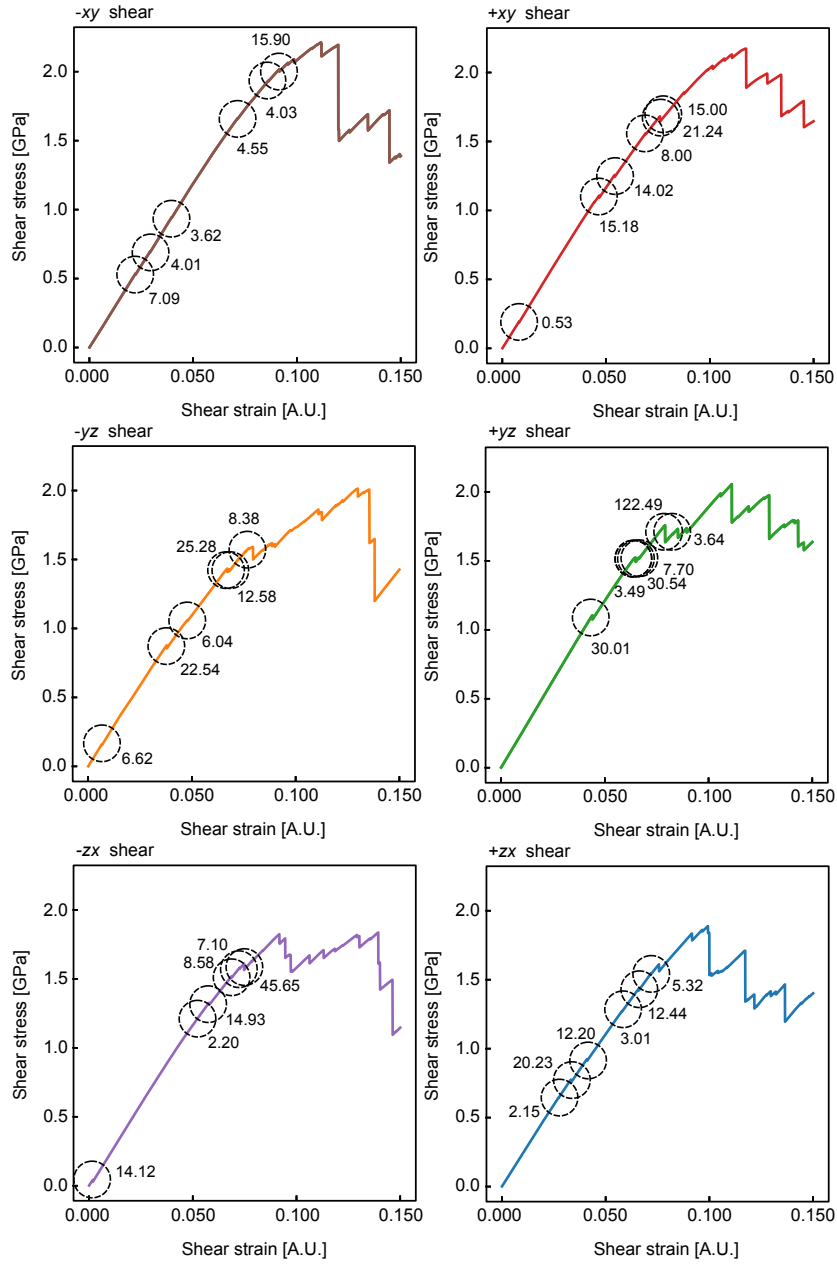


FIG. 5. Stress-strain curves obtained by AQS simulation and 36 stress-drop events considered. Each circle represents the position of the event, whose magnitude of stress drop [MPa] is also described.

local stress drops[49], local shear elasticity[50], von Mises strain, atomic displacements[51], and soft modes obtained through Hessian diagonalization[52]. Among these D_{\min}^2 has been particularly widely used. However, this method suffers from significant problems. In defining the non-affine displacement it is assumed that the affine strain is uniform, whereas the actual stress field is rather inhomogeneous in space. For instance, when an STZ is activated, local shear softening occurs, producing an elastic field around the STZ[2, 53]. Furthermore, to identify the STZ, a threshold value for D_{\min}^2 is set[54]. However, the choice of this value significantly affects the spatial distribution of the deformation elements as shown later, introducing large ambiguity. In order to elucidate the deformation mechanism, in this work we take a different approach and re-examine the definition of the deformation zones, such as STZs.

In the frozen atom analysis, we start with the atomic configuration just a step before a cooperative deformation event (see Fig. 1a). Then, after applying an affine deformation that will result in the deformation event, we artificially “freeze” an atom, and relax the rest during the relaxation process. If the cooperative motion ceases as a result of this freezing, we identify this atom as belonging to the atomic group we define as the STZ core, because the movement of this atom is essential for the deformation event to take place. Figures 6 and 7 present 12 events under $-xy$ and $+xy$ shear as examples, illustrating results similar to those in Fig. 1. Note that the center of the gravity of the atomic groups under cooperative motion is centered in these cells. Consistent with the results in the main text, the D_f parameter is obtained following the procedure described in Fig.1. Additionally, changes in D_{\min}^2 and von Mises stress are calculated by determining atomic displacements or differences in atomic von Mises stress before and after relaxation at the strain step where the event occurs. In all cases, the D_f parameter histogram successfully isolates deformation units that exhibit cooperative motion. Similar results were obtained for the other 24 cases not shown here. Uniquely defining STZ cores enables the calculation of their local physical properties. Figure 8 exemplifies the evolution of average atomic energy and von Mises stress within each STZ core during the AQS process. Atomic energy is computed using the EAM potential, while von Mises stress is derived from the average stress components within each STZ core. The response of individual STZ cores to shear strain at the system level varies significantly, exhibiting distinct behaviors across different cores. Furthermore, the activation of one STZ core strongly influences the properties of others. Even in regions that

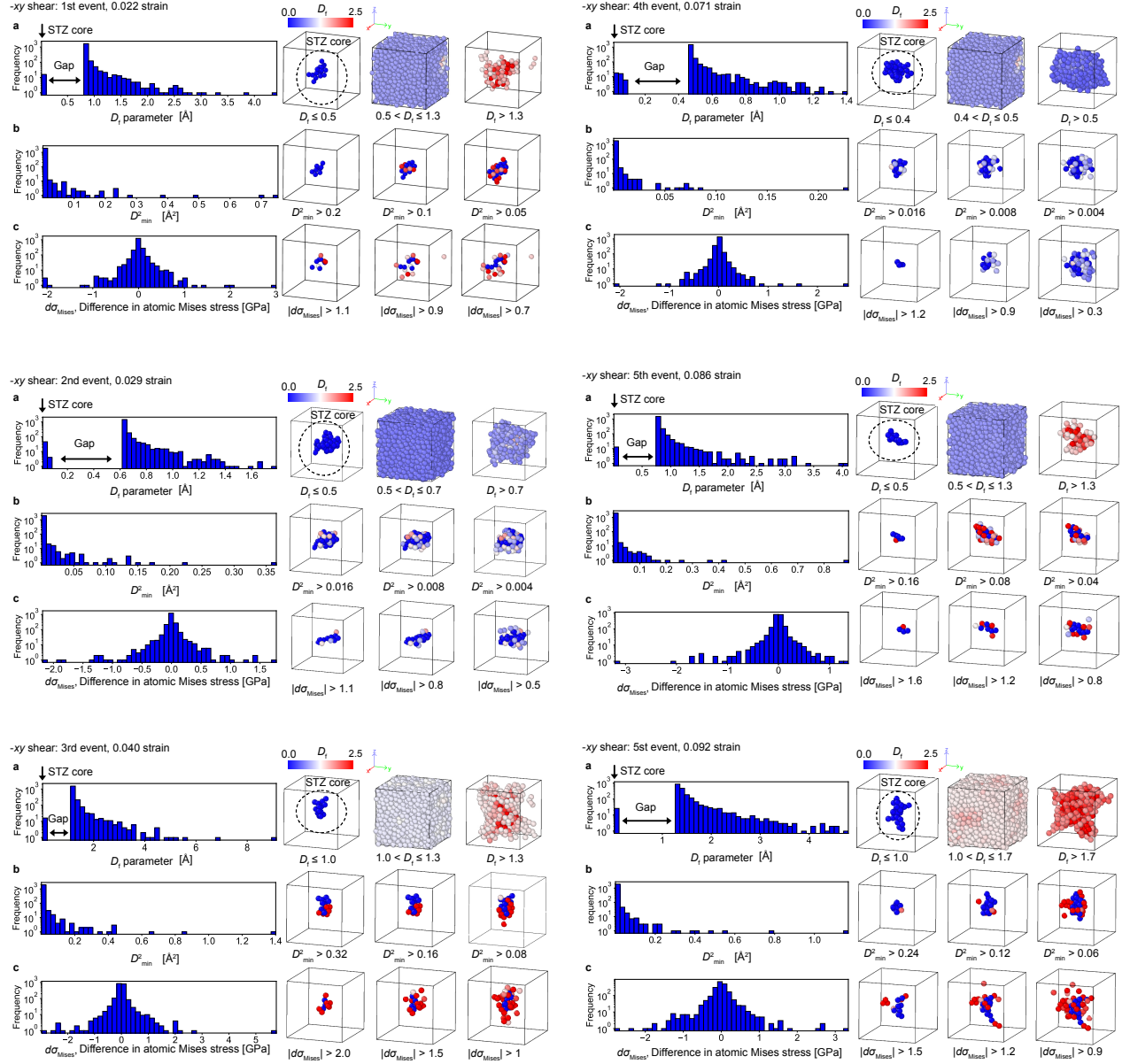


FIG. 6. Same as FIG. 1, with the six cases of $-xy$ direction. For details, refer to the caption of FIG. 1 in the main text.

appear to undergo elastic deformation between stress-drop events, local STZ core responses deviate considerably from the averaged behavior inferred from system-wide values. These findings demonstrate that physical quantities within STZ cores exhibit inherently nonlinear and transient characteristics.

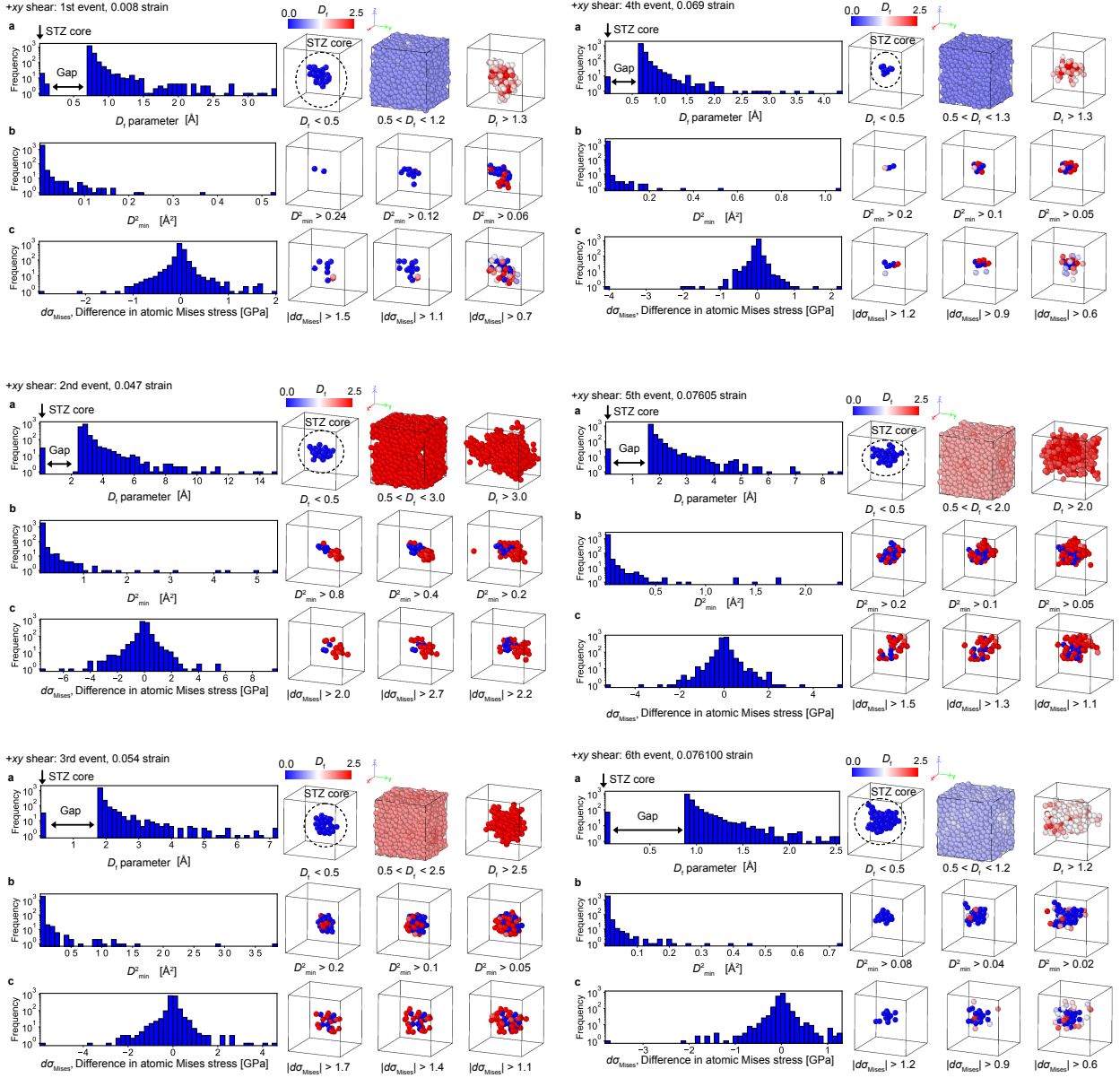


FIG. 7. Same as FIG. 1, with the six cases of +xy direction. For details, refer to the caption of FIG. 1 in the main text.

Local configurational excitation

Local Configurational Excitation (LCE) represents the reconfiguration of atomic bonding networks, as illustrated in Fig. 9, and has been discussed in the literature as a mechanism that determines the macroscopic viscosity of high-temperature liquids on an atomic level[30]. When LCE occurs—signified by the breaking and forming of atomic bonds—the balance of internal forces changes, leading to alterations in atomic-level stress. Additionally, atoms

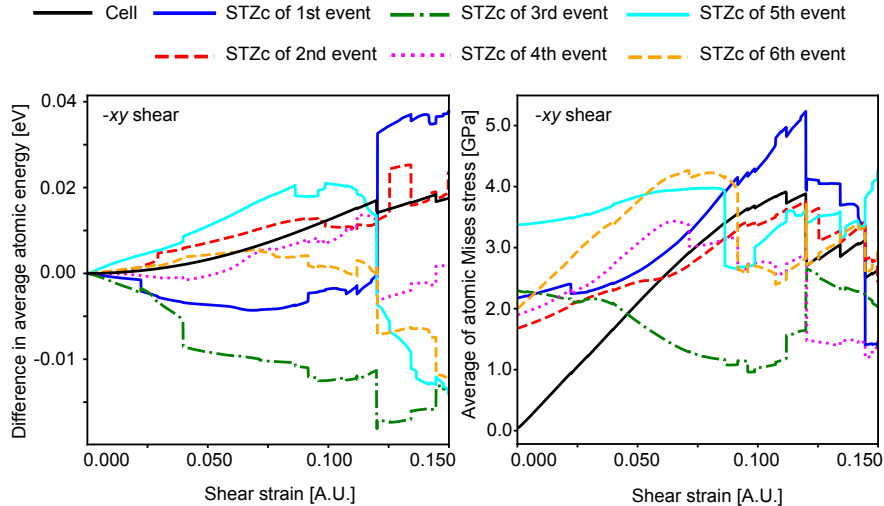


FIG. 8. Comparison of the evolution of average atomic energy (left) and stress state (right) for each STZ core in the $-xy$ shear case. The stress state is represented by the von Mises stress, calculated from the average stress components within each STZ core. System-averaged values are also shown for reference, highlighting the deviation of individual STZ cores from the overall material response.

displace to establish a new equilibrium. Thus, LCE is the phenomenon itself, driving the observed changes. Associated stress relaxation events and atomic displacements are not separate processes but are direct consequences of LCE.

In this study, to examine the relationship between cooperative motion identified by the D_f parameter and LCE, we analyzed the extent to which atoms undergoing LCE were included in groups exhibiting cooperative motion. The results are shown in Fig. 4a of the main text. Determining atomic bonding network reconfiguration is challenging in molecular dynamics; however, we assessed it by tracking atoms entering or leaving the first neighbor shell, following the method outlined in the literature [3] (see Fig. 9). Specifically, for configurations before structural relaxation in stress drop events, we first determined bond presence-whether atoms were in the first neighbor shell-using the pair density function. In this study, Zr-Zr, Cu-Cu, and Zr-Cu bonds were considered part of the first neighbor shell if their interatomic distances were within 4.35 Å, 3.05 Å, and 3.75 Å, respectively. Bond breaking was defined as an atom moving outside the first neighbor shell with an interatomic distance increase beyond a set threshold after relaxation, whereas bond formation was defined as an atom moving into the first neighbor shell with a decrease in interatomic distance beyond the same

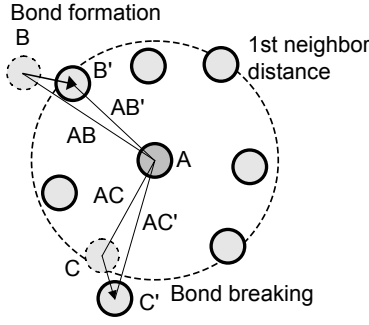


FIG. 9. Modification of local atomic connectivity due to bond formation and breaking.

threshold. The threshold was set at 0.075 \AA for this study. We evaluated the total bond breakings and formations per atom across 36 events (totaling 72,000 samples) and generated the histogram shown in Fig. 4.

LCE analysis is useful for capturing cascade events. Figure 10 presents the histograms of the D_f parameter and the atomic structures of STZ cores, atoms involved in LCE, and atoms with large non-affine displacements for five cases where a cascade is likely to have occurred among the 36 stress-drop events considered in this study. The LCE analysis and non-affine deformation capture atomic groups distinct from the STZ cores, suggesting that cascades are driven by the STZ cores. A notable feature was observed in the histogram of the D_f parameter: a small group of atoms appears just before the peak corresponding to the majority of atoms not involved in STZ core activation. Since frozen atom analysis can, in principle, capture only the initial STZ core, this secondary atomic group is not directly detectable. However, its presence suggests the existence of a second STZ core, whose activation is suppressed when the motion of its constituent atoms is frozen. This observation leads to the following scenario for cascade formation: an STZ core induces non-affine deformation via the LCE it contains, which subsequently triggers another STZ core. This chain reaction, with each step serving as an elementary process, ultimately results in an avalanche that drives large-scale plastic deformation.

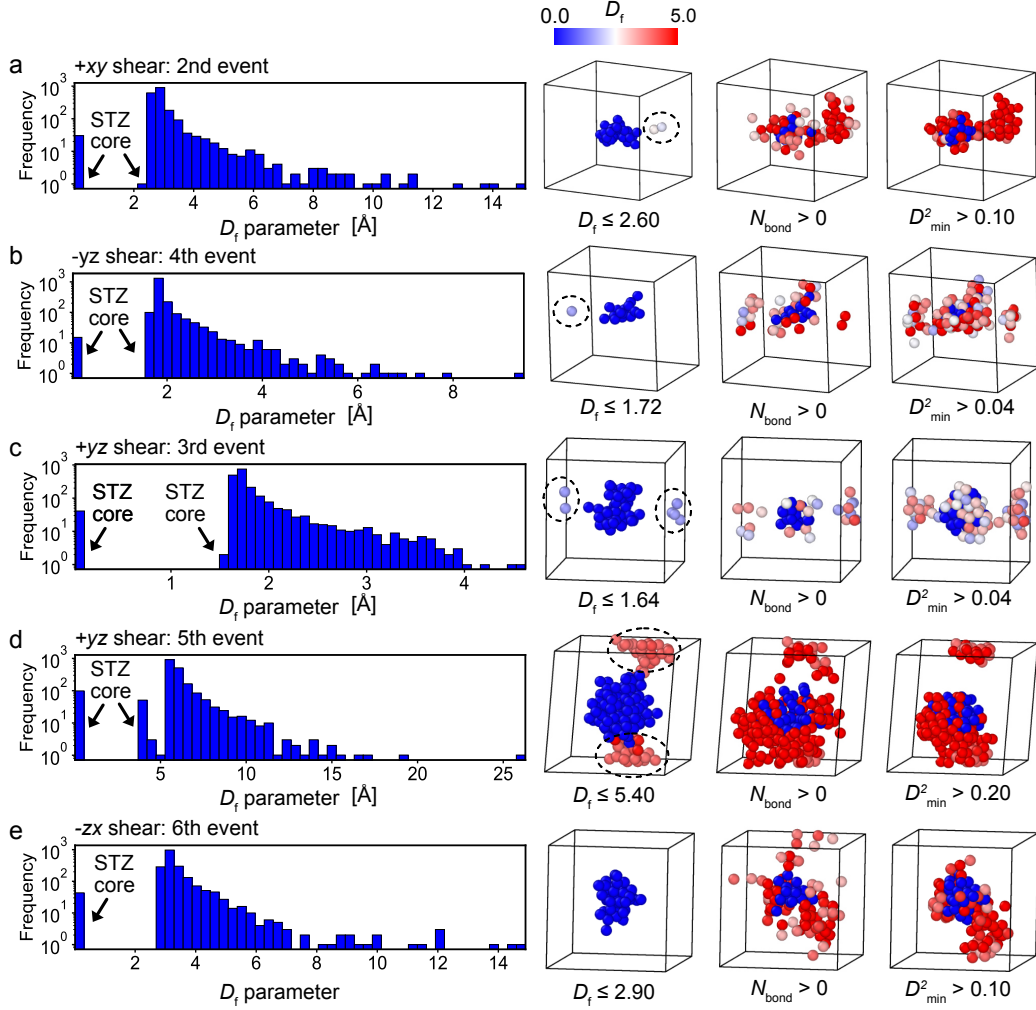


FIG. 10. Logarithmic histograms of the D_f parameter in cascade events. The histograms include STZ core atoms, LCE-related atoms, and atoms with large non-affine displacements. Dashed circles indicate additional STZ core that appear to be driven by another STZ core, identified by adjusting the D_f parameter threshold. Note that the system is under periodic boundary conditions: the triggered STZ cores actually belong to a single group.

Data availability

All data included in this article are available upon request to the corresponding author.

- [1] A. Greer, Y. Cheng, and E. Ma, Shear bands in metallic glasses, *Materials Science and Engineering: R: Reports* **74**, 71 (2013).
- [2] A. Nicolas, E. E. Ferrero, K. Martens, and J.-L. Barrat, Deformation and flow of amorphous solids: Insights from elastoplastic models, *Reviews of Modern Physics* **90**, 045006 (2018).
- [3] D. Richard, M. Ozawa, S. Patinet, E. Stanifer, B. Shang, S. A. Ridout, B. Xu, G. Zhang, P. K. Morse, J.-L. Barrat, L. Berthier, M. L. Falk, P. Guan, A. J. Liu, K. Martens, S. Sastry, D. Vandembroucq, E. Lerner, and M. L. Manning, Predicting plasticity in disordered solids from structural indicators, *Physical Review Materials* **4**, 113609 (2020).
- [4] N. Hansen, Hall–Petch relation and boundary strengthening, *Scripta Materialia* **51**, 801 (2004).
- [5] M. Meyers, A. Mishra, and D. Benson, Mechanical properties of nanocrystalline materials, *Progress in Materials Science* **51**, 427 (2006).
- [6] W. L. Johnson and K. Samwer, A Universal Criterion for Plastic Yielding of Metallic Glasses with a $(T / T_g)^{2/3}$ Temperature Dependence, *Physical Review Letters* **95**, 195501 (2005).
- [7] A. Argon and H. Kuo, Plastic flow in a disordered bubble raft (an analog of a metallic glass), *Materials Science and Engineering* **39**, 101 (1979).
- [8] F. Delogu, Effects of compression cycles on the atomic mobility in metallic glasses, *Physical Review B* **79**, 064205 (2009).
- [9] Z. Y. Liu, G. Wang, K. C. Chan, J. L. Ren, Y. J. Huang, X. L. Bian, X. H. Xu, D. S. Zhang, Y. L. Gao, and Q. J. Zhai, Temperature dependent dynamics transition of intermittent plastic flow in a metallic glass. II. Dynamics analysis, *Journal of Applied Physics* **114**, 033521 (2013).
- [10] B. S. Shang, M. Z. Li, Y. G. Yao, Y. J. Lu, and W. H. Wang, Evolution of atomic rearrangements in deformation in metallic glasses, *Physical Review E* **90**, 042303 (2014).
- [11] M. L. and B. Sen Gupta, Characteristics and correlations of nonaffine particle displacements in the plastic deformation of athermal amorphous materials, *Soft Matter* **18**, 8626 (2022).
- [12] G. Adam and J. H. Gibbs, On the Temperature Dependence of Cooperative Relaxation Properties in Glass-Forming Liquids, *The Journal of Chemical Physics* **43**, 139 (1965).

- [13] M. H. Cohen and G. S. Grest, The nature of the glass transition, *Journal of Non-Crystalline Solids* **61–62**, 749 (1984).
- [14] F. Blackburn, M. T. Cicerone, G. Hietpas, P. A. Wagner, and M. Ediger, Cooperative motion in fragile liquids near the glass transition: Probe reorientation in o-terphenyl and polystyrene, *Journal of Non-Crystalline Solids* **172–174**, 256 (1994).
- [15] C. Donati, J. F. Douglas, W. Kob, S. J. Plimpton, P. H. Poole, and S. C. Glotzer, Stringlike Cooperative Motion in a Supercooled Liquid, *Physical Review Letters* **80**, 2338 (1998).
- [16] H. Zhang, C. Zhong, J. F. Douglas, X. Wang, Q. Cao, D. Zhang, and J.-Z. Jiang, Role of string-like collective atomic motion on diffusion and structural relaxation in glass forming Cu-Zr alloys, *The Journal of Chemical Physics* **142**, 164506 (2015).
- [17] A. Jaiswal, S. O’Keeffe, R. Mills, A. Podlesynak, G. Ehlers, W. Dmowski, K. Lokshin, J. Stevick, T. Egami, and Y. Zhang, Onset of Cooperative Dynamics in an Equilibrium Glass-Forming Metallic Liquid, *The Journal of Physical Chemistry B* **120**, 1142 (2016).
- [18] M. L. Falk and J. S. Langer, Dynamics of viscoplastic deformation in amorphous solids, *Physical Review E* **57**, 7192 (1998).
- [19] J. P. Sethna, K. A. Dahmen, and C. R. Myers, Crackling noise, *Nature* **410**, 242 (2001).
- [20] J. Antonaglia, W. J. Wright, X. Gu, R. R. Byer, T. C. Hufnagel, M. LeBlanc, J. T. Uhl, and K. A. Dahmen, Bulk Metallic Glasses Deform via Slip Avalanches, *Physical Review Letters* **112**, 155501 (2014).
- [21] J. Antonaglia, X. Xie, G. Schwarz, M. Wraith, J. Qiao, Y. Zhang, P. K. Liaw, J. T. Uhl, and K. A. Dahmen, Tuned Critical Avalanche Scaling in Bulk Metallic Glasses, *Scientific Reports* **4**, 4382 (2014).
- [22] D. L. Malandro and D. J. Lacks, Molecular-Level Mechanical Instabilities and Enhanced Self-Diffusion in Flowing Liquids, *Physical Review Letters* **81**, 5576 (1998).
- [23] C. E. Maloney and A. Lemaître, Amorphous systems in athermal, quasistatic shear, *Physical Review E* **74**, 016118 (2006).
- [24] L. Berthier and W. Kob, Static point-to-set correlations in glass-forming liquids, *Physical Review E* **85**, 011102 (2012).
- [25] A. Stukowski, Visualization and analysis of atomistic simulation data with OVITO—the open visualization tool, *Modelling and Simulation in Materials Science and Engineering* **18**, 015012 (2009).

- [26] Y. Fan, T. Iwashita, and T. Egami, Evolution of elastic heterogeneity during aging in metallic glasses, *Physical Review E* **89**, 062313 (2014).
- [27] Y. Cheng and E. Ma, Atomic-level structure and structure–property relationship in metallic glasses, *Progress in Materials Science* **56**, 379 (2011).
- [28] T. Egami and D. Srolovitz, Local structural fluctuations in amorphous and liquid metals: A simple theory of the glass transition, *Journal of Physics F: Metal Physics* **12**, 2141 (1982).
- [29] C. K. C. Lieou and T. Egami, Relevance of structural defects to the mechanism of mechanical deformation in metallic glasses, *Scientific Reports* **13**, 15979 (2023).
- [30] T. Iwashita, D. M. Nicholson, and T. Egami, Elementary Excitations and Crossover Phenomenon in Liquids, *Physical Review Letters* **110**, 205504 (2013).
- [31] J. S. Langer, Dynamics of shear-transformation zones in amorphous plasticity: Formulation in terms of an effective disorder temperature, *Physical Review E* **70**, 041502 (2004).
- [32] T. Iwashita and T. Egami, Atomic mechanism of flow in simple liquids under shear, *Physical Review Letters* **108**, 196001 (2012).
- [33] K. A. Dahmen, Y. Ben-Zion, and J. T. Uhl, Micromechanical Model for Deformation in Solids with Universal Predictions for Stress-Strain Curves and Slip Avalanches, *Physical Review Letters* **102**, 175501 (2009).
- [34] K. A. Dahmen, Y. Ben-Zion, and J. T. Uhl, A simple analytic theory for the statistics of avalanches in sheared granular materials, *Nature Physics* **7**, 554 (2011).
- [35] J. T. Uhl, S. Pathak, D. Schorlemmer, X. Liu, R. Swindeman, B. A. W. Brinkman, M. LeBlanc, G. Tsekenis, N. Friedman, R. Behringer, D. Denisov, P. Schall, X. Gu, W. J. Wright, T. Hufnagel, A. Jennings, J. R. Greer, P. K. Liaw, T. Becker, G. Dresen, and K. A. Dahmen, Universal Quake Statistics: From Compressed Nanocrystals to Earthquakes, *Scientific Reports* **5**, 16493 (2015).
- [36] A. P. Thompson, H. M. Aktulga, R. Berger, D. S. Bolintineanu, W. M. Brown, P. S. Crozier, P. J. In 'T Veld, A. Kohlmeyer, S. G. Moore, T. D. Nguyen, R. Shan, M. J. Stevens, J. Tranchida, C. Trott, and S. J. Plimpton, LAMMPS - a flexible simulation tool for particle-based materials modeling at the atomic, meso, and continuum scales, *Computer Physics Communications* **271**, 108171 (2022).
- [37] Y. Q. Cheng, E. Ma, and H. W. Sheng, Atomic Level Structure in Multicomponent Bulk Metallic Glass, *Physical Review Letters* **102**, 245501 (2009).

- [38] S. Nosé, A unified formulation of the constant temperature molecular dynamics methods, *The Journal of chemical physics* **81**, 511 (1984).
- [39] W. G. Hoover, Canonical dynamics: Equilibrium phase-space distributions, *Physical Review A* **31**, 1695 (1985).
- [40] T. Nakamura, S. Kawamoto, and W. Shinoda, Precise calculation of the local pressure tensor in Cartesian and spherical coordinates in LAMMPS, *Computer Physics Communications* **190**, 120 (2015).
- [41] D. Wei, J. Yang, M.-Q. Jiang, B.-C. Wei, Y.-J. Wang, and L.-H. Dai, Revisiting the structure–property relationship of metallic glasses: Common spatial correlation revealed as a hidden rule, *Physical Review B* **99**, 014115 (2019).
- [42] I. Lobzenko, Y. Shiihara, T. Iwashita, and T. Egami, Shear Softening in a Metallic Glass: First-Principles Local-Stress Analysis, *Physical Review Letters* **124**, 085503 (2020).
- [43] Z.-Y. Yang, D. Wei, A. Zaccone, and Y.-J. Wang, Machine-learning integrated glassy defect from an intricate configurational-thermodynamic-dynamic space, *Physical Review B* **104**, 064108 (2021).
- [44] E. D. Cubuk, S. S. Schoenholz, J. M. Rieser, B. D. Malone, J. Rottler, D. J. Durian, E. Kaxiras, and A. J. Liu, Identifying Structural Flow Defects in Disordered Solids Using Machine-Learning Methods, *Physical Review Letters* **114**, 108001 (2015).
- [45] V. Bapst, T. Keck, A. Grabska-Barwińska, C. Donner, E. D. Cubuk, S. S. Schoenholz, A. Obika, A. W. R. Nelson, T. Back, D. Hassabis, and P. Kohli, Unveiling the predictive power of static structure in glassy systems, *Nature Physics* **16**, 448 (2020).
- [46] M. Baggioli, I. Kriuchevskiy, T. W. Sirk, and A. Zaccone, Plasticity in Amorphous Solids Is Mediated by Topological Defects in the Displacement Field, *Physical Review Letters* **127**, 015501 (2021).
- [47] M. Wakeda, Y. Shibutani, S. Ogata, and J. Park, Relationship between local geometrical factors and mechanical properties for Cu–Zr amorphous alloys, *Intermetallics* **15**, 139 (2007).
- [48] W. Jin, A. Datye, U. D. Schwarz, M. D. Shattuck, and C. S. O’Hern, Using delaunay triangularization to characterize non-affine displacement fields during athermal, quasistatic deformation of amorphous solids, *Soft Matter* **17**, 8612 (2021).
- [49] I. Lobzenko, T. Tsuru, Y. Shiihara, and T. Iwashita, First-principles atomic level stresses: Application to a metallic glass under shear, *Materials Research Express* **10**, 085201 (2023).

- [50] M. Tsamados, A. Tanguy, C. Goldenberg, and J.-L. Barrat, Local elasticity map and plasticity in a model Lennard-Jones glass, *Physical Review E* **80**, 026112 (2009).
- [51] D. Şopu, A. Stukowski, M. Stoica, and S. Scudino, Atomic-Level Processes of Shear Band Nucleation in Metallic Glasses, *Physical Review Letters* **119**, 195503 (2017).
- [52] D. Richard, G. Kapteijns, J. A. Giannini, M. L. Manning, and E. Lerner, Simple and Broadly Applicable Definition of Shear Transformation Zones, *Physical Review Letters* **126**, 015501 (2021).
- [53] R. Dasgupta, H. G. E. Hentschel, and I. Procaccia, Microscopic Mechanism of Shear Bands in Amorphous Solids, *Physical Review Letters* **109**, 255502 (2012).
- [54] Z. Fan and E. Ma, Predicting orientation-dependent plastic susceptibility from static structure in amorphous solids via deep learning, *Nature Communications* **12**, 1506 (2021).

Acknowledgement

This work was supported by Grant-in-Aid for Transformative Research Areas B, “Rheology of Disordered Structures: Establishing Anankeon Dynamics”, JSPS KAKENHI Grant Number 22B206, 22H05041, 22H05042, 22H05040. T. E. was supported by the U.S. Department of Energy, Office of Science, Basic Energy Sciences, Materials Sciences and Engineering Division.

Author contributions

Y.S. and T. I. conceived the research. Y. S. developed the modeling framework. Y.S. and T.I. performed the simulations and conducted the data analysis. Y.S. and T.E. wrote the manuscript. N. A. and Y. T. provided advice on the physics of the system. All the authors discussed the results and revised the manuscript.

Competing interests

The authors declare no competing interests.

Additional information

Correspondence and requests for materials should be addressed to Yoshinori Shihara, Takuya Iwashita, or Takeshi Egami.